Electron Exchange in Dissociative Excitation of Molecular Hydrogen using Polarized Electrons

J. F. Williams and D. H. Yu

Center for Atomic, Molecular and Surface Physics, School of Physics, University of Western Australia, Perth, Western Australia 6009, Australia

(Received 4 November 2003; published 11 August 2004)

The effects of electron exchange and spin orbit interaction in dissociative excitation processes in H_2 molecules have been explored using excitation by polarized electrons. Observations of the circular and linear Stokes polarizations of the Balmer-alpha photons determined the alignment and orientation of the excited atomic hydrogen atoms, the excited molecular states, and the dissociative excitation processes via predissociation with short and long range transitions.

DOI: 10.1103/PhysRevLett.93.073201 PACS numbers: 34.80.Gs

This Letter reports the first measurements using incident polarized electrons to observe the linear and circular polarization of Balmer-alpha radiation from dissociative excitation of molecular hydrogen. We determine the effects of electron exchange and the spin-orbit interaction [1] as well as electron configuration and the importance of predissociation. The timeliness of this study arises from the rapidly increasing use of fluorescence spectroscopy to identify, for example, the symmetry and rotational motion of large molecules [2] as well as the energy transfer to and from large molecules in liquids and membranes [3]. It can trace scattering dynamics within femtoseconds [4], quantify the association of labeled molecules with proteins [5], and enable testing DNA sequencing, fragment analysis, and immunoassays [6]. Most of these applications attach a fluorophore dye to selected parts of a macromolecule, excite the fluorophore with dipole radiation, and observe the fluorescence and its linear polarization. However, they usually do not access the information from electron exchange and spin-orbit interaction.

In this Letter, we observe Balmer-alpha radiation from the dissociated hydrogen atoms as the natural choice for study since many of the fluorophores and complex biomolecules contain hydrogen and there are many observations of the dissociative excitation of molecular hydrogen from fast photofragment spectroscopy [7], momentum spectroscopy of metastable atoms [8], time-dependent fluorescence intensities after pulsed synchrotron excitation [9], and photodissociation of doubly excited states [10], for example. However, they are photon impact experiments with dipole selection rules. Only the fast neutral beam [11] and unpolarized electron impact [12] studies indicate the importance of higher triplet states and electron exchange. In spite of this widespread use of fluorescence, these experiments have not determined the magnetic sublevel populations or the orientation of the electron charge cloud of the excited states or the importance of electron exchange and the spin-orbit interaction. Even though it is strongly suggested, for example, from ''dissociated fast atom'' spectroscopy [13], that angular momentum coupling within the molecule is one of the strongest depolarizing factors of the anisotropy of the fluorescent atoms, those effects were restricted by dipole selection rules. The use of anisotropy parameters was suggested [13] to reveal intramolecular structure, but not followed. Here we study molecular hydrogen as the simplest illustrative case. The significance of the present work is that polarized incident electrons, i.e., with controlled angular momentum, induce polarization of Balmer-alpha radiation from the dissociation process and enable identification of dissociation pathways not subject to dipole selection rules and the deduction of angular momentum coupling effects in molecular dissociation mechanisms.

A previous Letter [1] showed how electron exchange and spin-orbit effects could be observed separately, unambiguously, and quantifiably for excitation with incident spin-polarized electrons, with selected scattering dynamics and geometry, and with observation of the polarization of the radiated photons from single neon atoms with LS coupling. We apply that approach here to show how these fundamentally significant aspects have been observed in the fluorescence spectroscopy of relatively simple hydrogen molecules. To obtain this information we need to explain our observational method and how the results are interpreted.

The principles and the apparatus have been described in detail elsewhere for single atoms [1], and theory [14] extends the basic concepts to simple molecules. Briefly, the Stokes P_3 parameter may be nonzero due to either exchange or spin-orbit effects, and the Stokes P_2 parameter may be nonzero if the excited state is not well LS coupled or if spin-orbit forces are not negligible during the collision. We use incident spin-polarized electrons whose axial spin and momentum vectors define planar symmetry, so that measurements of the Stokes polarization parameters P_i $(i = 1, 2, 3)$ of the emitted radiation, normal to that plane and integrated over the unobserved electron scattering angles, give finer details of the excitation process [1]. The P_i are defined by the observed photon intensities where

$P_1 = [I(0°) - I(90°)]/I$, $P_2 = [I(45°) - I(135°)]/I$, and $P_3 = [I(\sigma^-) - I(\sigma^+)]/I$ where I is the total intensity, $I(\theta)$ is the photon intensity with the transmission axis of the polarizer at an angle θ with respect to the electron beam direction z, and $I(\sigma^+)$ and $I(\sigma^-)$ are the intensities of the photons with positive and negative helicity, respectively. With this normalization, the Stokes parameters are absolute quantities independent of total intensity variations.

For incident unpolarized electrons only axial symmetry is defined and angle-integrated Stokes parameters give zero values for P_2 and P_3 while P_1 may be nonzero. However, with transversely polarized electrons, the momentum and spin vectors define a symmetry plane, and nonzero values of P_2 and P_3 can be observed. The linear polarization P_1, i.e., the alignment of the electron charge cloud, has the same value regardless of the electron polarization. Whether the linear polarization P_2 and the circular polarization P_3 are actually zero, positive, or negative depends on the detailed collision mechanisms. Our experimental scattering geometry was chosen so that angular momentum transfer was detected only along the direction of light observation. The orbital angular momentum transfer averaged to zero due to the nonobservation of the scattered electrons; i.e., the observed effects were integrated over all scattering angles. Then angular momentum is transferred from the initial spin angular momentum through the spin-orbit interaction and by electron exchange, which can be identified through the values of P_2 and P_3 [1].

Briefly, the measurements were based on single particle scattering with crossed beams of molecular hydrogen and up to 76% polarized electrons, photoemitted from the (100) surface of a strained GaAs crystal by circularly polarized 830 nm diode laser photons. The intensity and polarization of the Balmer-alpha (656.8 nm) radiation from the molecules were determined using a liquid crystal variable retarder, 1 nm FWHM filter, and single-particle counting photomultiplier.

The measured Stokes parameters of the Balmer-alpha radiation from the dissociated H_2 are shown in Fig. 1 for energies within 2 eV of threshold. Four aspects require comment and the last two require analysis. First, checks on the validity of the measurements showed, for example, as in Fig. 1, that unpolarized electrons produced zero values of P_2 and P_3, whereas different initial electron spin polarizations of 32% and 75% produced identical values of P_3 after normalization to each other. Second, near the threshold for the production of radiation, the large uncertainty in the first several data points arises from the definition of the Stokes parameters as the sum and differences of very small intensities. This aspect also causes the apparent different threshold energy for each of the P_i. When error bars are not visible they are smaller than the size of the data points. The raw data are intensities that were accumulated over several days to obtain this statistical accuracy. Third, all the P_i values observed

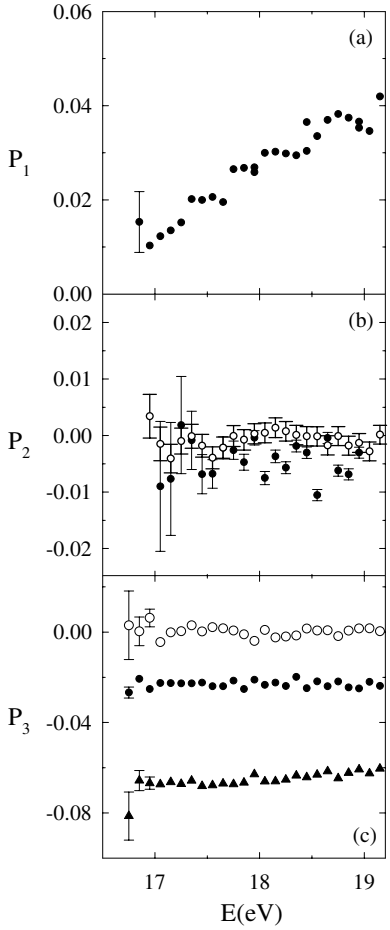

FIG. 1. The Stokes parameters P_1, P_2, and P_3 of the Balmer-alpha photons from H_2 are shown in (a), (b), and (c), respectively, for energies near threshold. Filled circles: 32% electron polarization; filled triangles: 75% electron polarization; open circles: unpolarized electrons.

using incident spin-polarized electrons are clearly different from zero, that is, polarization with alignment and orientation of the excited state electron charge cloud has been observed. Fourth, both P_1 and P_2 show "structure" outside 3 standard deviations of experimental uncertainty; i.e., the alignment P_1 increases from threshold, initially linearly with increasing energy, then with three steps, and the P_2 polarization shows several peaked values at approximately the same energies. In contrast, the orientation P_3 of the charge cloud has an approximately constant value and shows no structure within similar experimental uncertainties. This Letter now indicates the significance of these observations of spin effects on the populations of the $H(3\ell)$ levels by relating them to dissociating molecular states, the dissociation mechanisms, and angular momentum coupling.

The steady values of P_3 indicate significant exchange excitation and/or spin-orbit interaction for the 2 eV range studied and excitation of the $\pm m_j$ states required for these values of the orientation of the excited states. These features have not been observed previously for

molecules. A nonzero value of P_3 occurs since angular momentum is transferred parallel to the incident spin vector via electron exchange. Consequently, the role of triplet excited states is significant.

Figure 1 indicates uncertainty in locating the threshold for the P_2 parameter. A nonzero P_2 requires a planar rotation of the electron charge cloud, and it is observable when the spin-orbit interaction, here within the molecule, is effective during the excitation. The P_2 data indicate that the spin-orbit interaction clearly has sharp effects at selected energies that are close to the $n = 4$ (17.23 eV) and $n = 5$ (17.5 eV) dissociation thresholds and close to the $\prod^{1,3}$ and $^{1,3}\Delta$ (and higher) states which have an internal magnetic field in the direction of the internuclear axis resulting from the orbital motion of the electrons. The higher excited Rydberg-like states have faster moving nuclei, so that states with the same L, but different projections Λ of L on the internuclear axis, interact with increasing core rotation; the coupling of L to the internuclear axis becomes weaker, and Λ becomes a less good quantum number. The coupling changes from Hund's case (b) to (d); i.e., L uncouples from the internuclear axis and couples with the rotational axis, and, for example, this increases the spin-orbit interaction and increases magnetic sublevel populations. Here, the electron spin is perpendicular to the direction of detection, the perpendicular $\Delta\Lambda = \pm 1$ transition is favored from the ground state, and this increases the populations of the magnetic sublevels of the upper state and hence influence the Stokes parameters P_2 and P_3. It seems that at the peaks in P_2 the additional dissociation pathways open at large internuclear separations through the large number of repulsive states. Such states must couple rovibrationally with the potential energy curves of the $np\pi$ and $np\delta$ states, as shown in Fig. 2. Figure 1 also indicates that the mechanism is quickly damped within about 0.2 eV which is much wider than the apparent (but not measured) resolution for the spin-polarized electron beam.

Further evidence of the ways in which the states participate in dissociation is obtained from the study [15] with good 0.1 nm resolution of the Balmer-alpha decay using synchrotron radiation, in both absorption and emission. The fluorescence intensity was dominated by predissociation of the molecular $n = 4$, 5, $np\pi$ states with strong competition between molecular fluorescence, predissociation, and preionization. Well-defined structure from 16.57 to 17.19 eV on a continuum background indicated that most H(3ℓ) atoms were formed via predissociation. At large internuclear separations, at which higher relative velocities of the nuclei occurred, rearrangement of L states occurs through strong vibrational coupling of the $np\pi$ state with the $D(3p\pi)$ state and of the $np\sigma$ states with the $B''4p\sigma$ state and strong rotational coupling of the $D'(4p\pi)$ state with the $B''4p\sigma$ state, followed by predissociation through the repulsive parts of the D' and B'' states. This is consistent with the sharp

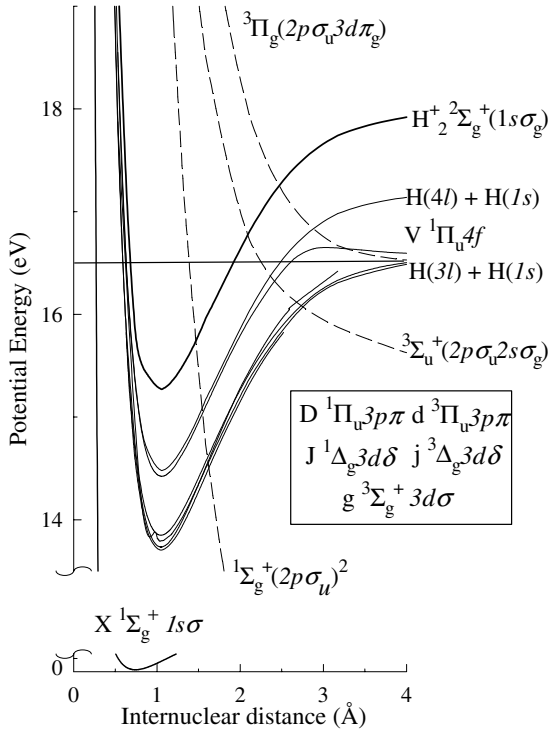

FIG. 2. The potential energy curves of H_2.

values of P_2. At small internuclear separations the 3ℓ populations are more localized and the intermediate state predissociates without any ℓ changing.

Since the $3s$ state cannot be polarized, any alignment and orientation is contained in the $3p$ and $3d$ states, and in turn from parent molecular states. Near threshold there are no published measurements using electron impact dissociation separating the $3s$, $3p$, and $3d$ fragments to give an estimate of their relative populations. The angular momentum population ratios of $3s$:$3p$:$3d$ after photoexcitation were estimated [16] as 1:4:4 at threshold, changing rapidly to 1:1:2 up to 0.25 eV and then constant over the next 2 eV. The reasons for these changes were not clear. Cascade effects would not account for the changes, and the background molecular radiation is negligible within the 1 nm optical passband. These ratios are in contrast to direct atomic excitation, which usually leads to more population in H($3p$) than in H($3s$) or H($3d$) states. It is clear that Fig. 1 shows the threshold for P_3 occurs at 16.62 ± 0.05 eV, which agrees within experimental uncertainty with 16.57 eV for the $3p\pi$ threshold from photon impact. This agreement also confirms the energy calibration via neon excitation spectra. Also, the fine and hyperfine structure effects and ortho-para differences [17] are not resolved.

The molecular states leading to dissociative Balmer-alpha decay after photon impact are well known [18,19] except just above the $n = 3$ and higher thresholds where the density of states is largest and where the present study is concerned. The better known potential energy curves shown in Fig. 2 indicate the singlet states,

which are characterized at the separated atom limit by $1\,^2S_g + 3\,^2S_g$, $1\,^2S_g + 3\,^2P_g$, $1\,^2S_g + 3\,^2D_g$ with the corresponding molecular electronic states $G\,^1\Sigma_g^+$, $^1\Sigma_u^+$ and $R\,\prod_g^1$, $D\,\prod_u^1$, $O\,^1\Sigma_g^+$, $B''B\,^1\Sigma_u^+$ and $J\,^1\Delta_g$, $^1\Delta_u$, $V\,\prod_u^1$, $P\,^1\Sigma_g^+$, $^1\Sigma_u^+$, respectively. Information on triplet states [18] is limited to the $g\,^3\Sigma_g^+ 3d\sigma$, $d\,\prod_u^3 3p\pi$, $J, j\,^{1,3}\Delta_g 3d\delta$ states indicated in Fig. 2. Often it is not clear whether single or multiple (mixed) configurations are required to characterize the excited state and the possible decay paths; for example, the $g\,^3\Sigma_g^+ 3d\sigma$ state produces a stronger $3s\sigma$ component at large internuclear separations R and a stronger $3d\sigma$ component at small R. Consequently, there is uncertainty even in interpreting high 0.02 nm resolution optical data and that is important when knowledge of the magnetic sublevels is required for interpreting the Stokes parameters.

Nevertheless, the potential energy curves and photon impact data [15] indicate that transitions at small and large internuclear separations are dominant. At small internuclear separations, the excitations to the repulsive part of the singly excited bound molecular Rydberg states dissociate into the correlated H($1s$) and H(3ℓ) states. Here the Born-Oppenheimer approximation is appropriate. In contrast at large internuclear separations, some states, for example, the Rydberg-like $V\,\prod_u^1 4f\pi$ singlet state, have a very small potential barrier through which the high vibrationally excited states may tunnel and then dissociate. Barrier heights ranging from 0.4 eV for the $i\,\prod_u^3 3d\pi$ state to 1.9 eV for the $m\,^3\Sigma_u^+ 4f\sigma$ state are known [18]. Also at large internuclear separations the singly excited states may decay by predissociation via a doubly excited state; for example, the $V\,\prod_u^1 4f\pi$ singly excited state is crossed by the $\prod_g^{1,3}(2p\sigma_u 3d\pi_g)$ doubly excited state. Other doubly excited states decaying asymptotically to the $n = 2$ level may, for example, interfere with degenerate levels and change the $n = 3$ flux.

It is noted that the $n = 3$ Balmer-alpha limit is higher than the H_2^+ ($v = 4$) level and the $n = 2$ Lyman-alpha limit is lower than the H_2^+ ($v = 0$) level and that all of the repulsive parts of the $n = 3, 4, \ldots, \infty$ potential curves lie below that of the H_2^+ curve. This means that there are many more dissociative channels available for Lyman-alpha predissociation, and for Balmer-alpha the long range $n = 4, 5, \ldots, \infty$ potentials will be relatively more important.

Also for the above states, laser studies [13] indicated that continuum excitation varies slowly with wavelength, whereas excitation of a predissociated level has a strong wavelength dependence. This mechanism seems quite general, and it is here postulated to occur similarly for Balmer alpha decay and would be consistent with our observations for polarized electron impact. For continuum state dissociation the excitation probability would be relatively slow, or flat at the present energy interval, while the predissociation mechanism leads to a relatively sharp excitation probability. Consequently, it is proposed that the steps in P_1 at 17.23 eV and 17.7 eV correspond with the $n = 4$ (17.23 eV) and $n = 5$ (17.5 eV) dissociation thresholds, respectively. The initial values of P_1 from 16.9 to 17.3 eV in Fig. 1 are consistent with predissociation and the remaining four plateau values consistent with dissociation via repulsive potentials. The evidence supports the opening of a new channel for populating the Balmer-alpha and its magnetic sublevels for each higher n value for the separated atoms, not via cascade but via predissociation through the repulsive potentials.

In conclusion, the technique of observing integral polarization has shown how polarized electron impact can identify predissociation pathways in molecular hydrogen where electron impact has not revealed such effects previously. The dissociative excitation of H_2 has produced small but significant alignment, orientation, and polarization of the H($n = 3$) electron charge cloud as observed in the Stokes P_i parameters. Small values of P_2, and structure in P_1 and P_2, indicate that configuration interaction played a role in the predissociation mechanisms. The integral Stokes parameters have identified spin-orbit effects in P_2 and electron exchange effects in P_3. Further studies using better electron energy resolution and coincidence outgoing particle detection are required for better identification of the dissociation pathways.

[1] D. H. Yu, P. A. Hayes, and J. F. Williams, Phys. Rev. Lett. **78**, 2724 (1997).
[2] R. Hall, B. Valeur, and G. Weber, Chem. Phys. Lett. **116**, 202 (1985).
[3] N. Duzgunes and J. Bentz, *Spectroscopic Membrane Probes* (CRC Press, Boca Raton, FL, 1988).
[4] S. Vaccari, S. Benci, and A. Peracchi, Biophys. Chem. **61**, 9 (1996).
[5] I. Hemmila, *Applications of Fluorescence in Immunoassays* (J. Wiley, New York, 1991), p. 107.
[6] J. Lakowicz, in *Advances in Fluorescence Sensing Technology V*, edited by J. Lakowicz and R Thompson (SPIE, Bellingham, WA, USA, 2001).
[7] C. J. Latimer *et al.*, J. Phys. B **29**, 6113 (1996).
[8] E. Sokell *et al.*, J. Phys. B **35**, 1393 (2002).
[9] M. Glass-Maujean *et al.*, J. Phys. B **34**, 5121 (2001).
[10] N. Kouchi, M. Ukai, and Y. Hatano, J. Phys. B **30**, 2319 (1997).
[11] W. Koot *et al.*, Phys. Rev. A **39**, 590 (1989).
[12] D. A. Vroom and F. J. de Heer, J. Chem. Phys. **50**, 573 (1969); **50**, 580 (1969).
[13] E. R. Wouters *et al.*, Chem. Phys. **218**, 309 (1997).
[14] K. Blum and H. Jakubowicz, J. Phys. B **11**, 909 (1978).
[15] P. Borrell *et al.*, J. Chem. Phys. **66**, 818 (1977).
[16] N. Terazawa *et al.*, J. Chem. Phys. **100**, 7036 (1994).
[17] J. R. Harries *et al.*, J. Phys. B **37**, 179 (2004).
[18] T. E. Sharp, At. Data **2**, 119 (1971).
[19] Y. Hatano, Phys. Rep. **313**, 109 (1999).